K03

Proceeding of 5th international Conference on Inverse Problems in Engineering: Theory and Practice Cambridge, UK, 11-15 th July 2005

ESTIMATION OF THE INITIAL TEMPERATURE PROFILE IN THE CHANNEL OF AN EXPERIMENTAL EXTRUSION DIE

M. KARKRI[1], Y. JARNY[1] and P. MOUSSEAU[2]
[1] *UMR CNRS 6607 Ecole Polytechnique de l'Université de Nantes 44306 cedex, France*
e-mail : mustapha.karkri@polytech.univ-nantes.fr ; m_karkri@hotmail.com
[2] *UMR CNRS 6144 IUT- Université de Nantes BP 539, 44475, France*

Abstract - This paper deals with the reconstruction of the inlet temperature profile of a melted polyethylene (PE) flowing through an extrusion die. The inverse heat transfer problem is formulated as an optimisation problem by considering both the energy and the Navier-Stokes equations. It is solved by using the conjugate gradient algorithm. Experimental results are presented and show the effect of the pressure drop combined with the viscous dissipation effect on the temperature profile along the channel die.

1. INTRODUCTION

During polymer extrusion, even after the melting zone, heat transfer takes an important place at the outlet of the extruder [1, 2]. The polymer flows through thin channel within the die. Due to high viscous dissipation and very low heat conductivity, the temperature profile can be quite sharp. Overheated area can be generated within the flow and degradation of the polymer could occur. For such creeping flow the temperature field is affected far downstream from the entrance of the die, so to predict accurately and to control the temperature rise, the inlet temperature profile has to be taken into account. However, due to the history in the extruder, the material temperature at the die entrance is rarely uniform. Hence the determination of this temperature profile is referred to as a boundary inverse heat transfer problem. There are numerous works on the initial temperature profile restoration, for example [3] estimated the inlet temperature profile in the laminar duct flow and subsequent investigations [4 - 6] examined various aspects of this problem. Recently, Hsu *et al*. [7] presented a two-dimensional inverse least squares method to estimate both inlet temperature and wall heat flux in a steady laminar flow in a circular duct. Huang and Chen [8] have solved a non-stationary Navier-Stokes equation, to provide coefficients for energy equation, but the velocity field does not depend on temperature. Gejadze and Jarny [9] have presented a detailed analysis of IHCP coupled problem, when the velocity field depends on temperature field through viscosity and Navier-Stokes equations for a non-Newtonian fluid. Recently, Nguyen and Prystay [10] estimated the initial temperature profile and its evolution in polymer processing using the surface temperature measurement and the conjugate gradient method was employed to search for the minimum of the functional.

In this work, the resolution of an inverse heat transfer problem is developed to estimate the temperature field within the polymer flow from temperature measurements taken inside the die wall. The solution is computed according to the classical Conjugate Gradient Method (CGM). An iterative numerical procedure is used to solve the direct, the adjoint and the sensitivity equations. The modelling equations for the fluid flow in the channel as well as for the heat flow within the melted polymer and the wall regions are solved simultaneously [11]. The melted polymer is considered as an incompressible pseudo-plastic fluid, and the flow is assumed to be steady and laminar. In a previous work [12] the sensitivity analysis led to important results to design the experimental die and to decide the location of the thermocouples within the die. The method was validated using numerically generated data for different thermal and flow conditions [13]. The algorithm is used here to predict the polymer temperature profile within an experimental die channel.

2. EXPERIMENTAL DEVICE

2.1 Extrusion Die

The main parts of the experimental extrusion die, described in Figures 1 and 2, are as follows:

- A rectangular channel $\left(2\times 30\text{mm}^2\right)$, is connected to the extruder outlet through a cone of length $l_c = 51\text{mm}$, the total channel length is $L_{ch} = 240\text{mm}.$
- The channel walls are made of four stainless blocks, instrumented by thermocouples (type K), the length, thickness and width of each block are $L = 200\text{mm}$, $H = 19\text{mm}$ and $l_b = 50\text{mm}$.
- Two electrical heater plates ensure the heating of the die on the upper and the lower faces.

- Two kinds of insulator are used to limit the heat side losses: a composite material and a porous foam-glass (thickness: 3 cm) surround the non-heated side surfaces of the die.

The pressure P_{mat} and the temperature T_{mat} of the polymer are measured near the channel entrance. The temperature of the extrusion die walls is measured in several places by using thermocouples (Chromel/Alumel, $\phi = 50\mu m$).

- 24 thermocouples are located close to the upper and lower faces of the channel ,
- 20 thermocouples close to both the heating plates
- 8 thermocouples are located at the outer face of the die

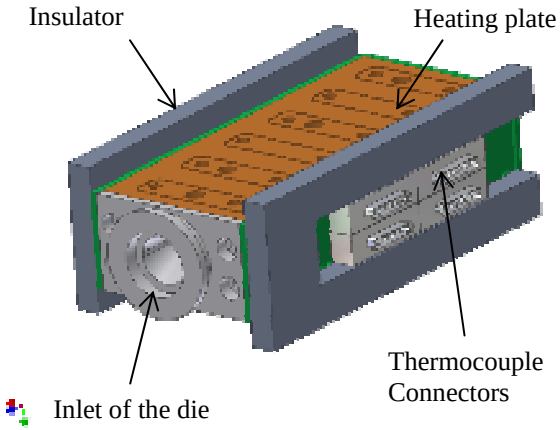

Figure 1 : Extrusion die (model 3D).

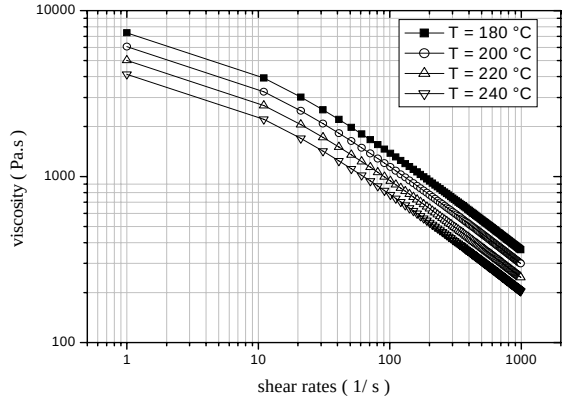

Figure 3 : Viscosity of PE melt.

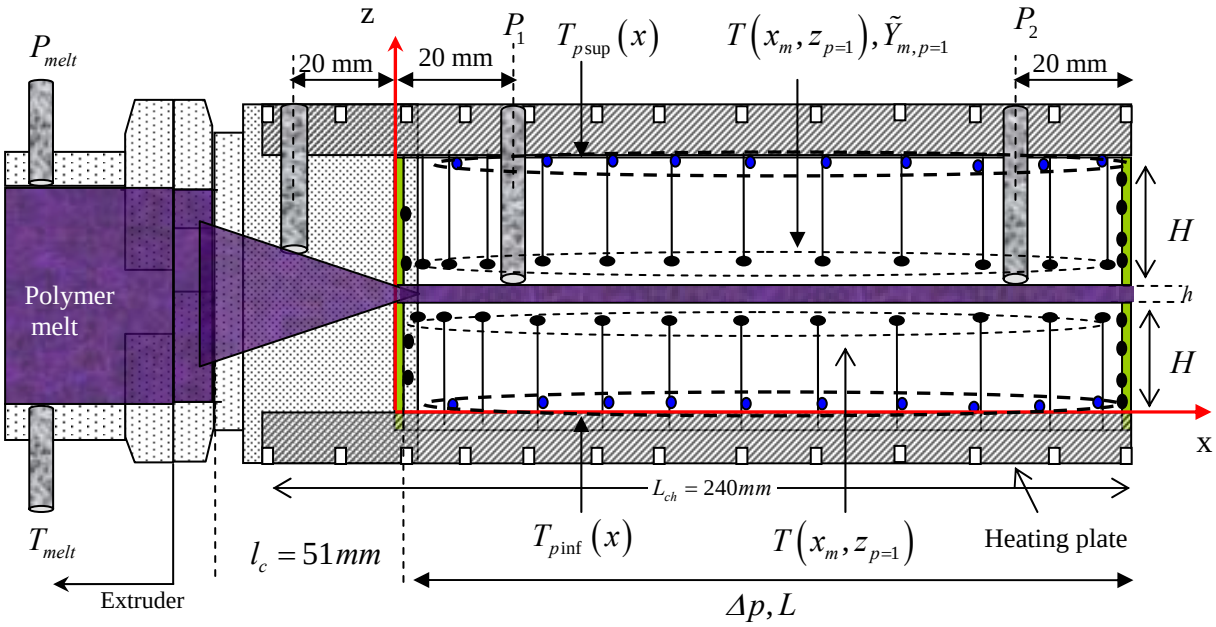

Figure 2 : Experimental die – sensor locations.

The thermophysical properties of the metallic die are assumed to be constant: the thermal conductivity is $\lambda_w = 16 W.(mK)^{-1}$, the heat capacity is $C_{pw} = 460 \;\; J.(kg\,K)^{-1}$ and the density is $\rho_w = 7800\,kg/m^3$.

2.2 Polymer Properties

The extrudated polymer used for the experiments is a polyethylene (PE Dowlex 2042E extrusion grade). The viscosity function $\eta(T, \dot{\gamma})$, is temperature and shear-rate dependent. The rheological properties were measured over the 450-510 K temperature range with shear rates varying from 0.1 s^{-1} to 1000s^{-1}. Determination of the

viscosity curve, Figure 3, over a wide range of shear rate values is essential for solving the flow eqns (2)-(12). The data measurements were fitted to the Cross WLF model.

$$\eta\left(T,\dot{\gamma}\right)=a\exp\left(bT\right)/\left[1+\left(\lambda\dot{\gamma}\right)^{1-n}\right] \tag{1}$$

The thermal and rheological parameters of the PE are given in Table 1.

Table 1: Thermal and rheological properties of PE Dowlex 2042E.

Thermal properties at T=220 °C		Rheological properties	
$\lambda_f\left(W.m^{-1}.K^{-1}\right)$	0.3	$a\ \left(Pa.s\right)$	54329
$C_{pf}\left(J.kg^{-1}.K^{-1}\right)$	2650	$b\ \left(K^{-1}\right)$	0.0095
$\rho_f\left(g.cm^{-3}\right)$	0.745	$\lambda\left(s^{-1}\right)$	0.1657
		n	0.36

2.3 Experimental Conditions and Procedure

All the experiments were carried out with a single-screw extruder (diameter 30 mm and length 780 mm). The maximum flow rate is 15 kg/h, and the maximum rotation speed 100 rpm. The flow rate was measured by weighing the mass of polymer exiting at the output of the die with an electronic balance. The pressure drop Δp along the channel die was also measured by using two pressure sensors located at the inlet and outlet die. The transducers are rated at up to 80 MPa and are interfaced with the control system, which displays the polymer pressures. The temperature of the upper and lower faces of the die were controlled by the heating units. Several tests on the PE Dowlex 2042E were carried out at different pressures from 10 to 25 MPa. Some experimental conditions are listed in the Table 2. Figures 6-9 show the temperature profiles measured within the die in the flow direction, both near the channel and the heating plates. The temperature is maximal at the die inlet and then decreases to reach a constant value, which was lower than the inlet melt temperature. At the die outlet the temperature profiles near the channel increase with the pressure drop. This observation is probably due to the shear heating effect. Figures 8 and 9 show the boundary conditions on the upper and lower faces.

Table 2: Tests conditions.

Tests	Screw rotation (rpm)	$T_{cinf}\left(°C\right)$	$T_{csup}\left(°C\right)$	$T_{mat}\left(°C\right)$	$P_{melt}\left(MPa\right)$	$\Delta p\left(MPa\right)$	$Q\left(g/s\right)$
1	10	200	200	201	9.9	8.8	0.15
2	19	200	200	201	15.6	13.9	0.29
3	26	200	200	202-201	20	17.7	0.43
4	37	200	200	201	25	20.3	0.53

3. MATHEMATICAL MODELING

A steady laminar flow model of an incompressible polymer is considered. Figure 4 shows the 2-D geometrical model ($\Omega=\Omega_1\cup\Omega_0$) of the extrusion die in a median plane parallel to the flow direction. The polymer melt enters the extrusion die at $x=0$ with a temperature profile $T_0\left(z\right)$. The velocity and the temperature fields are governed by the coupled equations of mass, momentum and energy, i.e.

$$\vec{\nabla}.\vec{U}=\vec{0}\quad\text{in}\quad\Omega_0 \tag{2}$$

$$\rho_f\left(\vec{U}.\vec{\nabla}\vec{U}\right)=-\vec{\nabla}p\ \ +\vec{\nabla}\left(\eta\vec{\nabla}\vec{U}\right)\quad\text{in}\quad\Omega_0 \tag{3}$$

$$\rho_f C_{pf}\vec{U}.\vec{\nabla}T=\vec{\nabla}.\left(\lambda_f\vec{\nabla}T\right)+F\left(T\right)+S_f\left(T\right)\ \text{in}\quad\Omega_0 \tag{4}$$

$$\vec{\nabla}.\left(\lambda_w\vec{\nabla}T\right)=S_w\left(T\right)\quad\text{in}\qquad\Omega_1 \tag{5}$$

The term $F(T)$ is due to viscous dissipation. According to the rheological behaviour, this term can take various forms. In our study, it is given by:

$$F(T) = \eta(T, \dot{\gamma})\dot{\gamma}^2 \tag{6}$$

The terms $S_f(T)$ and $S_w(T)$ are introduced for taking into account the heat losses through the connectors of the non-heated side face of the die.

$$S_{f,w}(x,z,T) = \frac{h_{eq}^{zone}}{l_{zone}}\left[T(x,z) - T_{amb}\right],\ (x,z) \in \Omega = \left[0, 0.2\right] \text{x} \left[0, 0.04\right] \tag{7}$$

where :

$h_{eq}^{zone}(x,z)$ = heat transfer coefficient for each zone, obtained by the thermal resistances calculated in the Oy direction. The spatial domain Ω is divided in 9 zones as shown in Figure 5.

l_{zone} = distance between the axis of the flow (Ox) and the end of each zones. T_{amb} = ambient temperature.

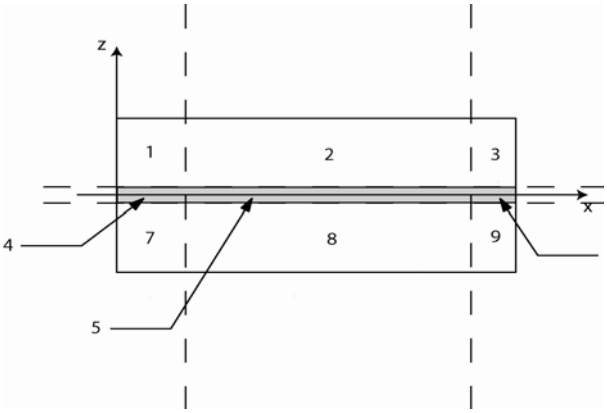

Figure 5: Lateral face of the extrusion die: locations of heat losses zones.

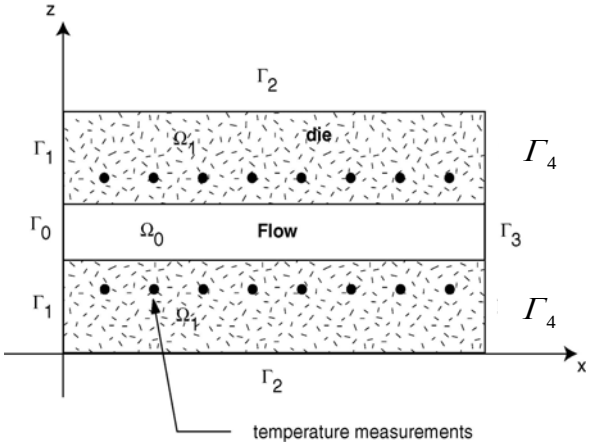

Figure 4 : Extrusion die / 2-D spatial domain.

The following boundary conditions are considered for the velocity field:

- At the inlet of the channel : $p = P_0$, $\dfrac{\partial u}{\partial x} = 0$ and $w = 0$ on Γ_0 (8)
- At the outlet : $p = P_L$, $\dfrac{\partial^2 u}{\partial x^2} = 0$ and $\dfrac{\partial w}{\partial x} = 0$ on Γ_3 (9)
- At the internal surface, the usual no-slip boundary condition : $\vec{U} = \vec{0}$ (10)

For the temperature field, the boundary conditions are taken as follows:

- At the channel entrance : $T = T_0(z)$ on Γ_0 (11)

The heat flux and the surface temperature of the die are fixed :

$$\lambda_f \frac{\partial T}{\partial \mathrm{n}} = 0 \quad \text{on} \quad \Gamma_3 \tag{12}$$

$$\lambda_w \frac{\partial T}{\partial \mathrm{n}} = 0 \ \text{on} \ \Gamma_1 \tag{13}$$

$$T = T_{p\,\mathrm{sup,inf}}(x) \ \text{on} \ \Gamma_2 \tag{14}$$

$$T = T_s(z) \ \text{on} \ \Gamma_4 \tag{15}$$

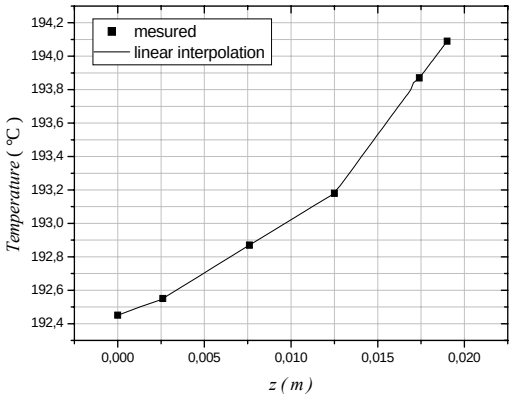

Figure 6: Measured temperature at the outer die face $T_s\left(x = 200mm, 0 < z \le 19\,mm\right)$.

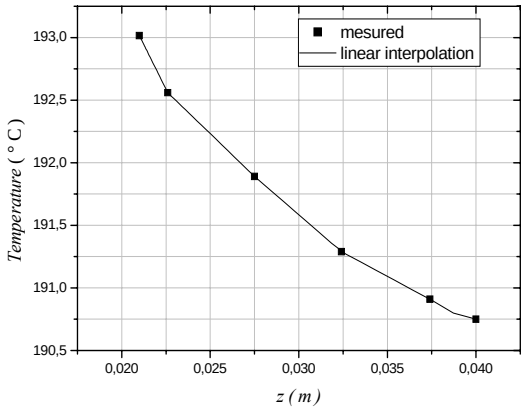

Figure 7: Measured temperature at the outer die face $T_s\left(x = 200mm, 21mm < z \le 40\,mm\right)$.

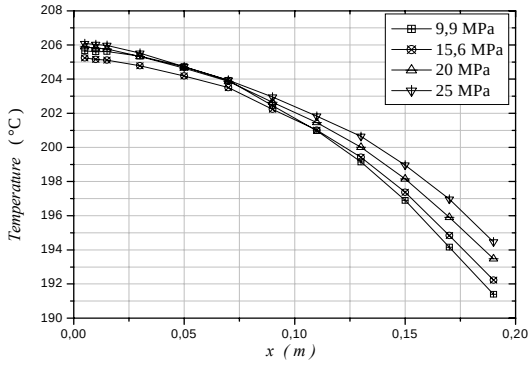

Figure 8: The measured temperature $\tilde{Y}_{m,p}$: Influence of the pressure drop.

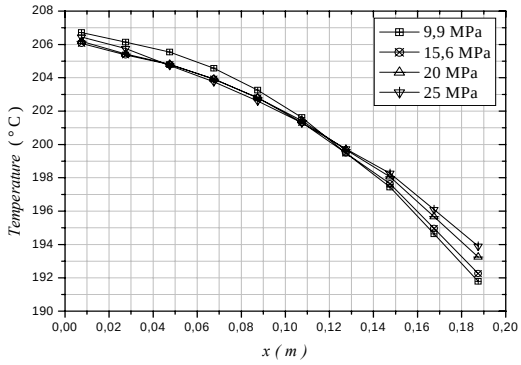

Figure 9: Temperature near the heating-plate : $T_{p\,\sup,\inf}\left(x\right)$.

4. INVERSE HEAT TRANSFER PROBLEM

The inlet temperature profile $T_0\left(z\right)$ has to be determined from the temperature $\tilde{Y}_{m,p}$ given by *Ns* sensors located inside the extrusion die at $\left(x_m\,,\,z_p\right),\ m = 1,...Ns/2\,,\ p = 1,2$.

The inverse problem is formulated by considering the following least square functional:

$$J\left(T_0\right) = \frac{1}{2}\sum_{p=1}^{2}\sum_{m=1}^{Ns/2}\left(T\left(x_m, z_p; T_0\right) - \tilde{Y}_{m,p}\right)^2 \qquad (16)$$

where $T\left(x_m, z_p; T_0\right)$ are the temperature computed from the direct problem equations, at the measurement locations, with the estimated inlet temperature profile $T_0\left(z\right)$.

The CGM was used to search for the minimum of the functional. This method has been well documented elsewhere [14, 15] and will not be repeated here. The method is based on the computation of the gradient of the functional, which is obtained by solving the sensitivity problem and the adjoint problem defined as follows.

4. 1 The Sensitivity Problem

In order to develop the sensitivity problem equations, a variation $\varepsilon\delta T_0$ of the inlet temperature profile is considered, and the resulting temperature is denoted $T^+ = T\left(x, z; T_0 + \varepsilon\delta T_0\right)$. The sensitivity is then defined by :

$$\theta = \underset{\varepsilon \to 0}{Lim} \frac{T^{+} - T(T_0)}{\varepsilon} \tag{17}$$

Developing the direct problem eqns (2)-(15) for $T(x,z;T_0)$ and $T(x,z;T_0+\varepsilon\delta T_0)$ and then subtracting the resulting expressions lead to :

$$\rho C_{Pf} \vec{U}.\vec{\nabla}\theta = \lambda_f \Delta(\theta) + \frac{\partial(F+S_f)}{\partial T}\theta \quad \text{in} \quad \Omega_0 \tag{18}$$

$$\lambda_w \frac{\partial \theta}{\partial n} = 0 \qquad \text{on} \quad \Gamma_1 \tag{19}$$

$$\lambda_f \frac{\partial \theta}{\partial n} = 0 \qquad \text{on} \quad \Gamma_3 \tag{20}$$

$$\theta = 0 \qquad \text{on} \quad \Gamma_2 \quad \text{and} \quad \Gamma_4 \tag{21}$$

$$\theta = \delta T_0 \qquad \text{on} \quad \Gamma_0 \tag{22}$$

$$\vec{\nabla}\left(\lambda_w \vec{\nabla}\theta\right) = \frac{\partial S_w}{\partial T}\theta \qquad \text{in} \quad \Omega_1 \tag{23}$$

where $\vec{U}$ is the direct problem velocity profile in the extrusion die.

4. 2 The Adjoint Problem

The following adjoint problem equations are obtained [14]:

$$\rho C_{Pf} \vec{U}.\vec{\nabla}\Psi + \lambda_f \Delta\Psi + \frac{\partial(F+S_f)}{\partial T}\Psi = \sum_{p=1}^{2} \sum_{m=1}^{Ns/2} \left(T(x_m, z_p; T_0) - \tilde{Y}_{m,p}\right) \delta_{x_m}(x)\, \delta_{z_p}(z) \text{ in } \Omega_0 \tag{24}$$

$$\Psi = 0 \quad \text{on} \quad \Gamma_0, \tag{25}$$

$$\lambda_w \frac{\partial \Psi}{\partial n} = 0 \quad \text{on} \quad \Gamma_1 \tag{26}$$

$$\Psi = 0 \quad \text{on} \quad \Gamma_2 \text{ and } \Gamma_4 \tag{27}$$

$$\lambda_f \frac{\partial \Psi}{\partial n} + \rho C_{Pf} \vec{U}.\vec{n}\,\Psi = 0 \quad \text{on} \quad \Gamma_3 \tag{28}$$

$$\vec{\nabla}\left(\lambda_w \vec{\nabla}\Psi\right) = \frac{\partial S_w}{\partial T}\Psi \qquad \text{in} \quad \Omega_1 \tag{29}$$

together with the gradient equation :

$$\vec{\nabla} J(T_0) = \lambda_f \left.\frac{\partial \Psi}{\partial n}\right|_{\Gamma_0} \tag{30}$$

5. RESULTS AND DISCUSSION

The computational technique used to solve the direct problem is based on a Finite Volume Method (FVM) discretization of the governing mass, momentum and energy equations. The system of the governing equations is discretized by employing the staggered grid for Marker and Cell (MAC) method. An augmented Lagrangian method [11] is used to compute the solution of the coupling velocity-pressure equations. The grids are non uniformly spaced in z direction. The mesh spacing is taken smaller near the channel. The grids in the principal direction of flow are uniformly spaced (200×160). This distribution was dictated by the desire to capture the details of the viscous dissipation, because the temperature rise occurs in the region very near the wall, the temperature rise remains very low in the centre of the channel die. The accuracy of the direct problem solution was studied in a previous paper [13]. The comparison between the numerical and the analytical solutions confirms that the selected grid is adequate. The same numerical method and grids are used to solve the adjoint and the sensitivity problem.

In order to examine the feasibility and then the accuracy of the inverse analysis for estimating the unknown inlet distribution temperature, by using the CGM, several numerical experiments including a constant function and a smooth function have been studied for the non-Newtonian flow in extrusion die [12].
In the present work, the inlet temperature profile is reconstructed for the test conditions n°3. Two solutions have been computed: one with the heat losses $S_{f,w}(x,z,T)$ equal to zero, the other one where $S_{f,w}(x,z,T)$ is given by the eqn (7), [14].
For case I ($S_{f,w}(x,z,T)=0$), the computation starts from the uniform guess $T_0^{n=0}(z)=470K$. In Figure 10, comparison is made between the initial temperature profile and the reconstructed temperature profile. It can be observed that the temperature is very high near the walls (260°C) and low in the channel center (130°C). The estimated profile is physically difficult to interpret. Figures 11 and 12 show the comparison between the measured and calculated temperature at polymer-walls interfaces and the evolution of the least square criterion. After 3 iterations the least square criterion remains constant.

For case II $\left(S_{f,w}(x,z,T)\neq 0\right)$, the computation starts from the uniform guess $T_0^{n=0}(z)=473K$. In Figure 13, comparison is made between the initial temperature profile and the reconstructed temperature profile. It can be observed that at the outlet of the channel, the temperature mean of the melt decreases, while the profile shows a maximum at the channel center. These observations result mainly of the low thermal conductivity of the melt and of the heat losses through the non-heated faces of the die. It is observed that when the number of iterations increases, the final value of the least square criterion decreases (Figure 15) and a reasonably inlet temperature solution is obtained after 5 iterations. Although the optimal number of iterations is difficult to be determined a priori, the plot of the iterative process, Figures 14 and 15, confirm the efficiency of the CGM and suggest that the optimal number of iterations is around 5, when the least square criterion J is close to the expected value: $J=N_s\sigma^2$, which leads here to $\sigma^2\approx 0.09/24\Rightarrow\sigma\approx 0.06°C$. This value of the standard deviation of the measurement noise is quite correct. This result should be compared (and to be confirmed) to that of the other experiments. The inlet temperature profile estimated at the iteration numbers 5 and 20 remains unchanged.

6. CONCLUSIONS

An inverse algorithm was developed to construct the inlet temperature profile of the melted polymer from the temperature data measured in the solid wall of the extrusion die. The reconstructed profile without heat losses is not realistic and a reasonable profile was obtained when we take into account the heat losses. This result needs to be verified for other pressure drops.

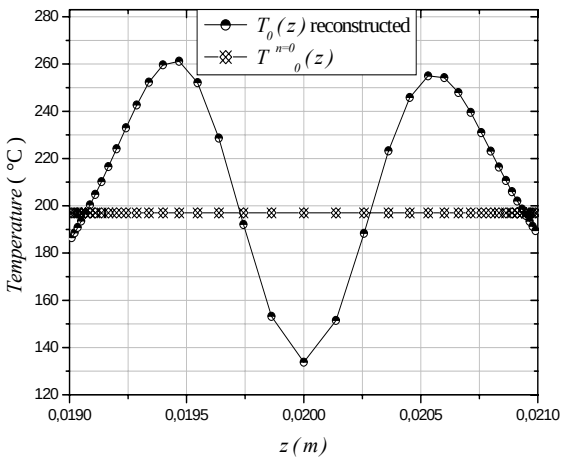

Figure 10 : Estimated inlet and outlet temperatures $P_{melt}=20MPa$, $S_{f,w}=0$.

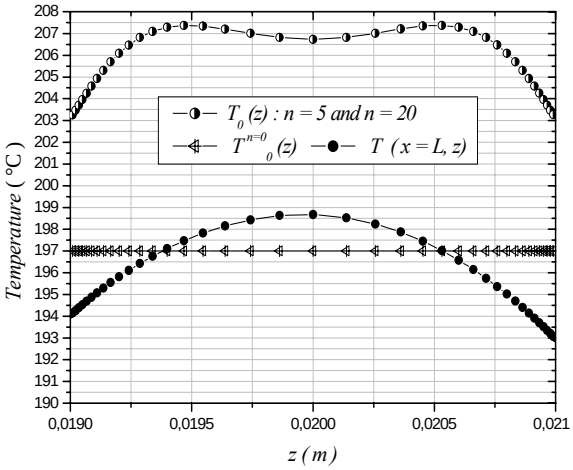

Figure 13: Estimated inlet and outlet temperatures $P_{melt}=20MPa$, $S_{f,w}\neq 0$.

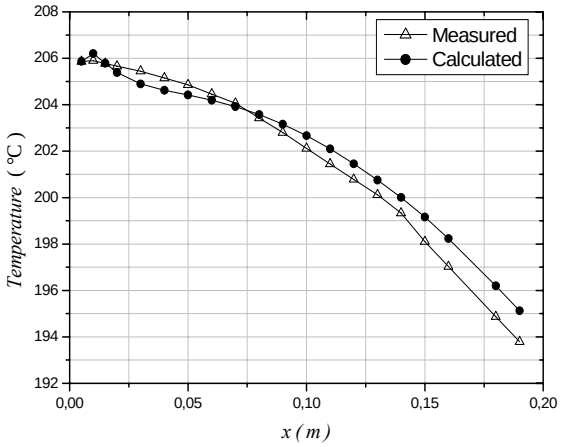

Figure 11 : The measured and calculated temperatures $\tilde{Y}_{m,p}$, $P_{melt} = 20MPa$, $S_{f,w} = 0$.

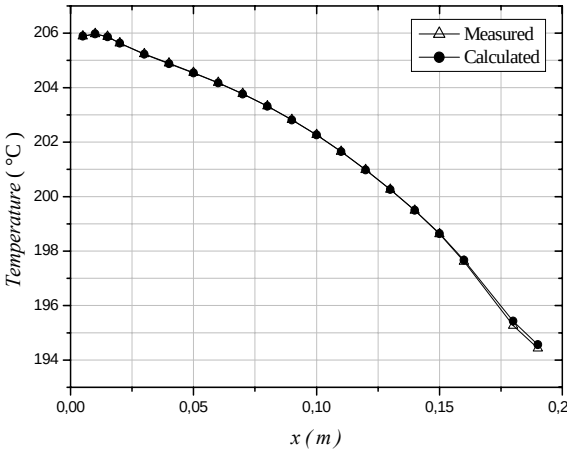

Figure 14: The measured and calculated temperatures $\tilde{Y}_{m,p}$, $P_{melt} = 20MPa$, $S_{f,w} \neq 0$.

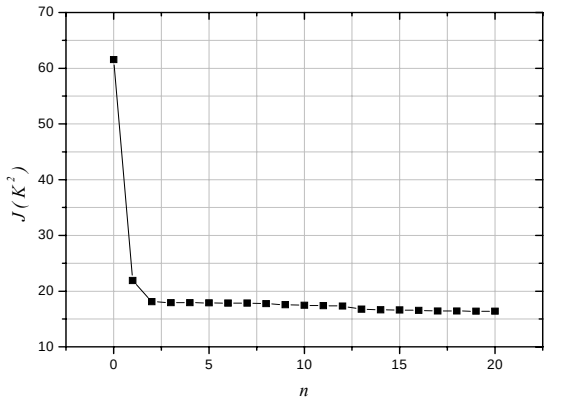

Figure 12 : Least square Criterion $J(T_0(z))$, $S_{f,w} = 0$.

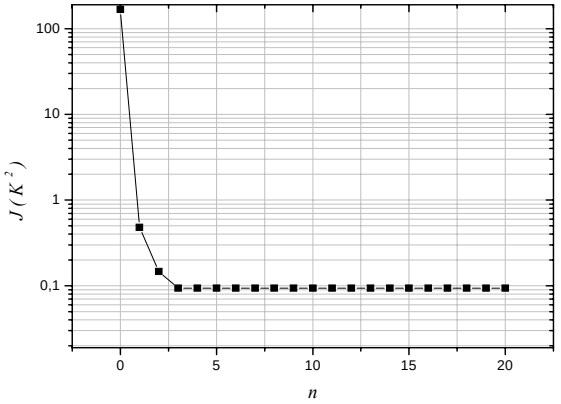

Figure 15 : Least square Criterion $J(T_0(z))$, $S_{f,w} \neq 0$.

NOMENCLATURE

Δp : pressure drop, $\Delta p = P_0 - P_L$

C_p : heat capacity

η : dynamic viscosity

F : source term of energy

T_0 : inlet temperature of the fluid

p^n : direction of descent at iteration *n*

J : functional to be minimised

$\tilde{Y}$: measured temperatures

l_c length of the die connector

L_{ch} : length of the heating-plate

Subscripts

m , p : sensor locations

P_0 : inlet pressure

P_L : outlet pressure

$\vec{U}$: velocity

u , w : axial and radial velocities

T : temperature

$\boldsymbol{n}$: vector normal

Ns : number of sensors

Superscripts

n : iteration number

Greek Symbols

$\dot{\gamma}$: shear rate

Ψ : adjoint variable

e : inlet die
s : outlet die
w : wall
f : fluid

θ : sensitivity variable
ρ : density
δ : Dirac delta function
Ω : spatial domain

REFERENCES

1. Z. Tadmor and C. G. Gogos, *Principles of Polymer Processing*, Wiley, New York, 1979.

2. J.F. Agassant, P. Avenas, P. Sergent and P. Carreau, *Polymer Processing, Principles and Molding*, Hanser Publishers, Munich, 1991.

3. F. C. Liu and M. N. Özisik, Estimation of inlet temperature profile in laminar duct flow. *Inverse Problems in Engineering* (1996) **3**, 131-141.

4. J. C. Bokar and M. N. Özisik, Inverse analysis for estimating the time varying inlet temperature in laminar flow inside a parallel plate duct. *Int. J. Heat Mass Transfer* (1995) **38,** 39-45.

5. C. H. Huang and M. N. Özisik, Inverse problem of determining unknown wall heat flux in laminar flow trough a parallel plate. *Numer. Heat Transfer* (1992) **21**, 55-70.

6. H. A. Machado and H. R. B. Orlande, Inverse problem for estimating the heat flux to a non-Newtonian fluid in a parallel plate channel. *J. Brazilian Soc. Mech. Sci.* (1998) **20**, 51-61.

7. P. T. Hsu, C. K. Chen and Y. T. Yang, A 2-D inverse method for simultaneous estimation of the Inlet temperature and wall heat flux in laminar circular duct flow. *Numer. Heat Transfer* (1989) **34**, 731-745.

8. C.-H. Huang and W.-C. Chen, A three-dimensional inverse forced convection problem in estimating surface heat flux by conjugate gradient method. *Int. J. Heat Mass Transfer* (2000) **43**, 3171-3181.

9. I. Gegadze and Y. Jarny, An inverse heat transfer problem for restoring the temperature field in a polymer melt flow through a narrow channel. *Int. J. Thermal Sci.* (2002) **41**, 528-535.

10. K. T. Nguyen and M. Prystay, An inverse method for estimation of the initial temperature profile and its pvolution in polymer processing. *Int. J. Heat Mass Transfer* (1998) **42**, 1969-1978.

11. http://www.enscpb.fr/master/Aquilon/.

12. M. Karkri, Y. Jarny and P. Mousseau, Inverse heat transfer analysis in a polymer melt flow within extrusion die, *Inverse Problem, Design and Optimisation Symposium*, Rio de Janerio, Brazil, 2004.

13. M. Karkri, Y. Jarny, P. Mousseau and R. Deterre, Thermique de l'écoulement d'un polymère pseudoplastique, *Acte du Congrès SFT*, Elsevier, 2003, pp. 667-672.

14. M. Karkri, *Heat Transfer in Steady Polymer Flow through an Extrusion Die: Thermal Metrology and Inverse Method*, PhD Thesis, Université de Nantes, 2004.

15. O. M. Alifanov, *Inverse Heat Transfer Problems*, Springer-Verlag, Berlin, 1994.